37-GHz Modulation via Resonance Tuning in Single-Mode Coherent Vertical-Cavity Laser Arrays

Stewart Thomas McKee Fryslie, *Student Member, IEEE*, Meng Peun Tan, *Member, IEEE*, Dominic Francis Siriani, Matthew Thomas Johnson, and Kent D. Choquette, *Fellow, IEEE*

***Abstract*— We show a significant improvement of modulation bandwidth from 2 × 1 photonic crystal vertical-cavity surface-emitting laser arrays. Control of injection bias conditions to array elements enables resonance tuning of each element with variation of the phase relation and coherence of the array, resulting in the ability to tailor the modulation response. A bandwidth of 37 GHz is obtained under highly single-mode coherent operation with narrow spectral width and increased output power while the laser array is biased at low current density. Lasers with such performance characteristics may greatly enhance high-rate data transfer in computer server, data center, and supercomputer applications with potentially long device lifetime.**

***Index Terms*— Modulation, surface-emitting lasers, phased arrays, semiconductor laser arrays.**

I. Introduction

VERTICAL-CAVITY surface-emitting lasers (VCSELs) possess characteristics such as low power consumption, circular beam output for efficient fiber coupling, low-cost manufacturability, and scalability in two-dimensional arrays. Therefore they have become the dominant source for optical data communication links in computer server, data center, and super computer applications. There have been several reports of VCSEL modulation rate in excess of 50 Gbps [1], [2] although these experiments have been into a few 10s of meter of fiber and require high current density. Modulation rate times distance products of 25 × 1 [3], 20 × 2 [4], and 1 × 10 [5] Gbps × km have been achieved using single mode or quasi-single mode VCSELs for reduced modal and chromatic dispersion. Transversely coupled dual VCSELs have recently been reported with small signal modulation bandwidth as high as 29 GHz and large signal operation of 36 Gbps, albeit in multi-mode or quasi-single mode operation [6]–[8]. The bandwidth improvement is reported to arise from photon-photon coupling [9]. To satisfy the need for optical data communications links requiring error-free transmission over long distances (>1 km) of fiber at high data rate (>20 Gbps), it is crucial to employ VCSELs with large modulation bandwidth, single mode or narrow spectral width, increased output power, and reliable operation.

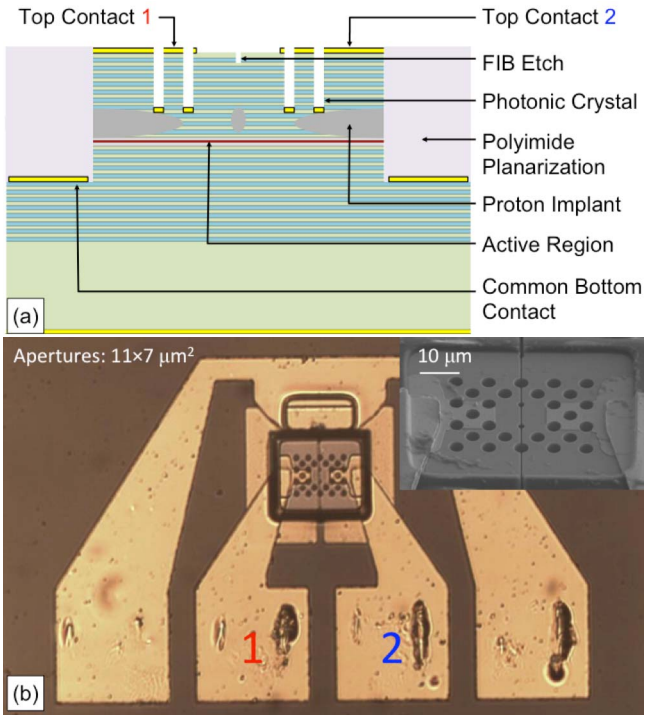

Fig. 1. (a) Cross-sectional sketch and (b) optical image with inset electron microscope image of 2 × 1 photonic crystal VCSEL array.

In this letter, we report controlled and reproducible bandwidth enhancement using 2 × 1 coherently coupled photonic crystal VCSEL arrays in single-mode coherent operation. Small signal bandwidth of 37 GHz (receiver limited) is obtained with side-mode suppression ratio (SMSR) of 40 dB and narrow RMS spectral width of 0.043 nm for the coherently coupled out-of-phase mode. Due to the coherent coupling in these arrays, the bandwidth enhancement is accompanied by an increased output power of >3.4 mW and is achieved at an operating current density of <8 kA/cm^2 [10].

II. Device Design & Fabrication

A cross-sectional sketch is shown in Fig. 1(a) and an optical image with a scanning electron micrograph inset of

Manuscript received August 7, 2014; revised November 14, 2014; accepted November 26, 2014. Date of publication December 4, 2014; date of current version January 28, 2015. This work was supported by Oracle Corporation, Redwood, CA, USA.

S. T. M. Fryslie and K. D. Choquette are with the Department of Electrical and Computer Engineering, University of Illinois at Urbana-Champaign, Champaign, IL 16820 USA (e-mail: fryslie2@illinois.edu; choquett@illinois.edu).

M. P. Tan is with Intel Corporation, Hillsboro, OR 97124 USA (e-mail: mengtanuiuc@gmail.com).

D. F. Siriani is with the MIT Lincoln Laboratory, Lexington, MA 02421 USA (e-mail: dominic.siriani@ll.mit.edu).

M. T. Johnson is with the U.S. Air Force, Colorado Springs, CO 80840 USA (e-mail: mtjohns2@illinois.edu).

Color versions of one or more of the figures in this letter are available online at http://ieeexplore.ieee.org.

Digital Object Identifier 10.1109/LPT.2014.2376959

the 2×1 photonic crystal VCSEL array is shown in Fig. 1(b). The 2×1 VCSEL arrays studied here are similar to those reported in [11]. As depicted in Fig. 1(a), the coherently coupled array is fabricated by combining a photonic crystal etched hole pattern with an ion implant-defined laser gain structure. The photonic crystal is a square lattice (6 μm period) of circular holes (diameters of 0.6 times period) with lattice defects defining the optical apertures of each array element. The lattice defects are designed such that there is not an etched hole directly between the two elements and with holes nearest the defect having reduced size (diameter of 0.3 times period) to enhance optical coupling. The photonic crystal provides stable index guiding for array elements and greater optical loss for higher order modes [12], [13]. The current apertures defined by ion-implantation are designed such that they overlap both the top metal contacts and the photonic crystal apertures with 140 μm^2 of conductive area and 2 μm of implanted separation between the elements. This structure enables strong coupling between array elements and stable out-of-phase operation under proper biasing conditions.

The VCSEL epitaxial material consists of 20 p-type top distributed Bragg reflector (DBR) mirror periods, 36 n-type bottom DBR mirror periods on an n-type GaAs substrate, and an active region with strained InGaAs quantum wells emitting nominally at 975 nm. Laser fabrication begins with the deposition, photolithographic patterning, and reactive-ion etching (RIE) of a SiO_2 etch mask for the photonic crystal and mesa. Before etching the photonic crystal and mesa by inductively coupled plasma (ICP) RIE, gain apertures aligned to the photonic crystal patterns are formed by photolithographic patterning of a mask and proton implantation. Subsequent are the depositions of n-type bottom contact and p-type top contacts, planarization using HD-4000 polyimide, and deposition of ground-signal-signal-ground (GSSG) coplanar interconnect metal contacts as seen in Fig. 1(b). In an additional step, the highly conductive top DBR period is bisected between the array elements by focused ion beam (FIB) etch to provide electrical isolation between top contacts and additional current confinement between array elements. Although helpful in controlling the behavior resulting in enhanced modulation bandwidth, the FIB etch is not necessary and could be avoided, for example, with a stacked ion implantation step [6]. Therefore the fabrication process requires only standard photolithographic and semiconductor manufacturing processes.

III. Experimental Results

DC current injection into the array elements is achieved with high-precision current sources biasing the sample via a high-speed GSSG probe. The modulation response and optical spectra are simultaneously measured as shown in Fig. 2(a) by use of a 1×2 fiber splitter, optical spectrum analyzer (OSA), high-speed photoreceiver with 25 GHz 3-dB bandwidth, and Agilent E8363C 40 GHz parameter network analyzer. The far-field profile is obtained from an LD8900 goniometric radiometer as shown in Figure 2(b). The setup is constructed such that the data acquisition portrayed in Fig. 2(a) can be quickly transitioned to that of Fig. 2(b) by simple adjustment.

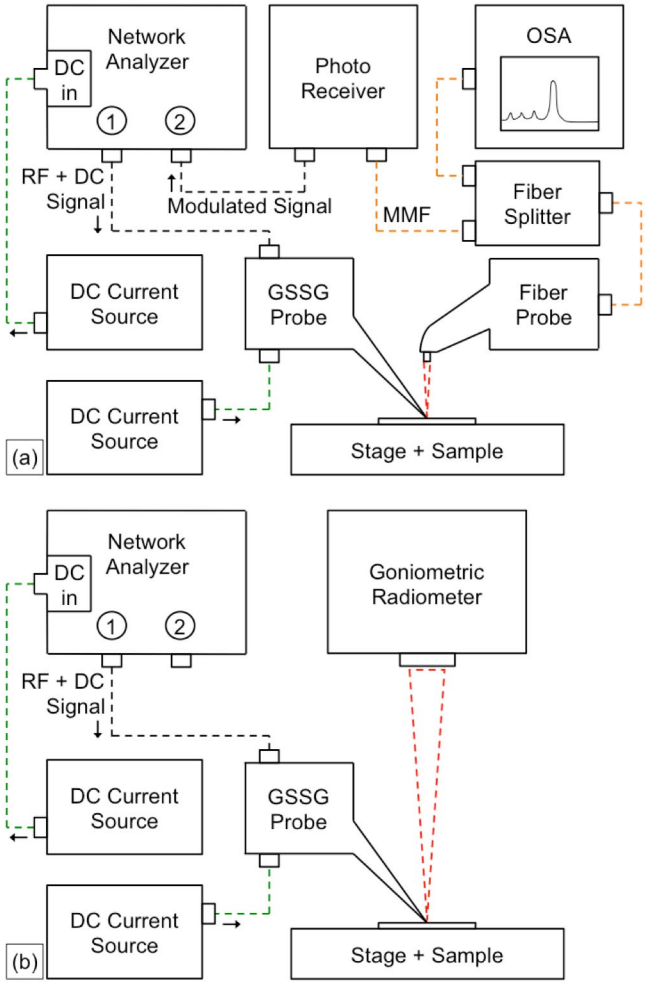

Fig. 2. Experimental setups to obtain (a) modulation response, spectra, and (b) far-field data.

This allows us to accurately measure the far-field profile and optical spectra that correspond to the modulation response.

Fig. 3 shows the output power and voltage versus current for the array under different biasing schemes. The voltage versus current data has been included to allow for estimates of resistance, power efficiency and compatibility with high-speed driver circuits. As shown in Fig. 3(a), there is a difference in the output power for each element biased separately indicating significant electrical isolation between array elements. Near-field observation also confirmed for biasing up to 8 mA, only the biased array element lases. By preferential current injection to one element with respect to the other, we change the cavity refractive index for that element through ohmic heating and electronic suppression [14], thus varying its natural resonance (confirmed by spatially resolved spectra measurements). In effect, by varying the bias we can tune the resonance of each element [14] as well as the phase relation and coherence of the array [15]. By electrically tuning Elements 1 and 2, we obtain highly single-mode emission with an "out-of-phase" mode throughout the coherent operation regime, one of which is apparent in Fig. 3(b) with 4.3 to 5.6 mA injected into Element 2. With sufficient detuning two clearly defined spectral peaks with a single broad Gaussian far-field are

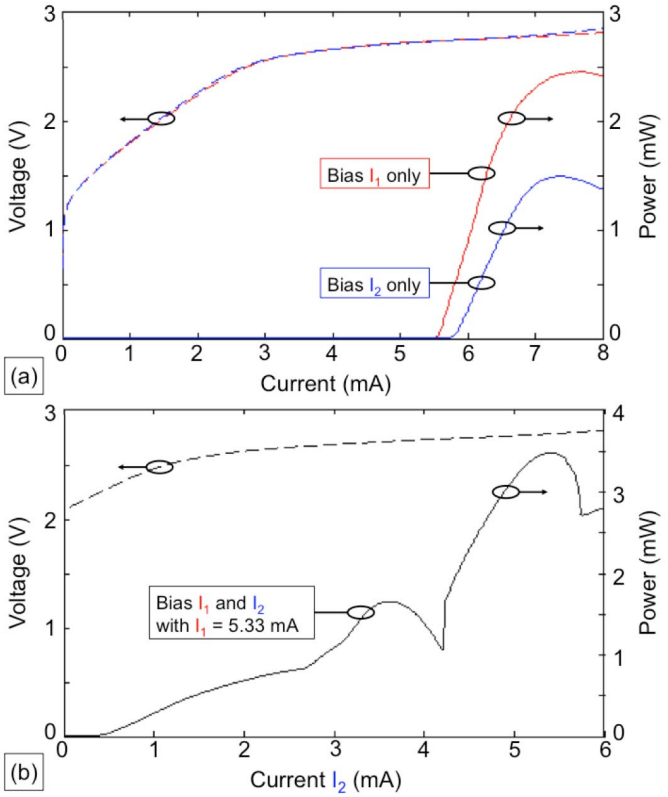

Fig. 3. Output power and voltage versus current for the 2×1 array under different bias conditions.

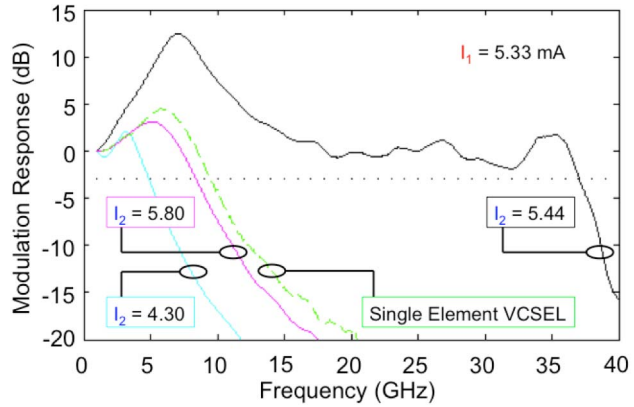

Fig. 4. Modulation response of the 2×1 VCSEL array under different bias conditions as well as that of a single element photonic crystal VCSEL from the same sample biased at I = 8 mA.

apparent when the elements become uncoupled and incoherent, in agreement with prior reports [15].

Fig. 4 shows the small signal modulation response of the 2×1 VCSEL array under different bias conditions. For reference the modulation response of a single element photonic crystal VCSEL from the same sample biased at I = 8 mA or about $4\times$ threshold current is included in Fig. 4. The network analyzer is set to input RF power of -10 dBm, with averaging in both time (50 sweeps) and frequency domain (2% smoothing), and low IF bandwidth of 5 kHz. By averaging over 50 sweeps we show that the behavior plotted in Fig. 4 is stable and reproducible. The current applied to Element 1 is modulated with a constant DC bias

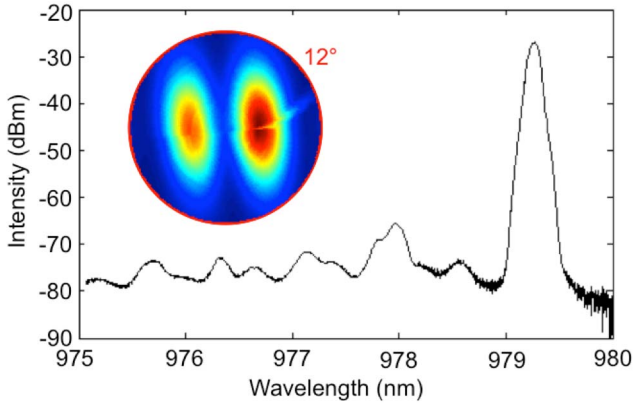

Fig. 5. Spectra of coherently coupled 2×1 VCSEL array under direct modulation giving bandwidth enhancement. The corresponding far-field intensity image inset shows out-of-phase coherent coupling.

$I_1 = 5.33$ mA (current resolution of ± 5 μA), while the DC bias, I_2, applied to Element 2 is varied in order to tune resonance and thus the phase relation and coupling between the two elements. As shown in Fig. 4, for bias values of I_2 producing incoherent array operation with the uncoupled resonance of Element 2 blue-detuned ($I_2 = 4.30$ mA) and red-detuned ($I_2 = 5.80$ mA) from that of Element 1, the modulation response of the 2×1 array is similar to that of an individual VCSEL. The maximum achieved 3-dB bandwidth is 37 GHz (limited by the photoreceiver bandwidth) obtained at injection currents of $I_1 = 5.33$ mA and $I_2 = 5.44$ mA. The simultaneously measured emission spectra and far field for the 2×1 array while producing this modulation response behavior is shown in Fig. 5. For this condition, Elements 1 and 2 are coherently coupled with 40 dB SMSR and narrow RMS spectral width of 0.043 nm (calculated according to the IEEE 802.3 Standard) for the coupled mode. In the far-field we observe two lobes with an on-axis null in between them, as in the inset of Figure 5, indicating out-of-phase coupling. The bias currents corresponding to those giving the maximum enhanced bandwidth produce an output power of >3.4 mW as shown in Fig. 3(b). The maximum enhanced bandwidth is achieved at an operating current density of <8 kA/cm^2 [7].

We have performed measurements on 2×1 arrays with different structural designs and from other epitaxial wafers for both 980 and 850 nm emission wavelengths. The measured bandwidth enhancement beyond 30 GHz has been observed from several arrays. Similar improvements in bandwidth enhancement have been observed from arrays emitting nominally at the 850 nm wavelength. Inconsistent bandwidth enhancement of lesser magnitude has been observed to occur serendipitously from arrays without electrical isolation between elements (e.g. without the FIB etch), showing that while unnecessary for producing bandwidth enhancement, electrical isolation is essential for its control and optimization through resonance tuning. Furthermore, it has been observed that while the bandwidth enhancement correlates with spectral detuning of the natural resonances of array elements emitting in a coherently coupled mode, the phase and strength of the coherent coupling play a role in determining the frequencies of additional resonances and

RF gain of those resonances in the modified modulation response. For a coherently coupled array emitting in the in-phase mode we have observed enhanced modulation bandwidth without a low frequency peak in the modulation response.

IV. Conclusion

In conclusion, we demonstrate that resonance detuning and variation of the phase relation and coherence of 2×1 photonic crystal VCSEL arrays can simultaneously achieve enhanced modulation response with narrow single-mode spectral width and relatively high output power while operating at low current density, all of which are desirable for reliable data transmission over large distances in fiber. The increased small signal bandwidth achieved over prior results from transversely coupled VCSELs [6]–[8] arises, in part, from the control of resonance frequency detuning in our coherent arrays, and the coherence in turn enables highly single mode operation at relatively high output power. In order to control the modulation bandwidth enhancement, other approaches for electrical isolation between array elements and/or different approaches for controlling the optical modes can be investigated. Larger arrays with different phase relationships between elements also could potentially allow for increased output power and further manipulation of the modulation response with more resonance frequencies and increased RF gain, thus further enhancing modulation bandwidth.

References

[1] D. Kuchta *et al.*, "64 Gb/s transmission over 57 m MMF using an NRZ modulated 850 nm VCSEL," in *Proc. Opt. Fiber Commun. Conf.*, San Francisco, CA, USA, Mar. 2014, pp. 1–3, paper Th3C.2.

[2] P. Westbergh, E. P. Haglund, E. Haglund, R. Safaisini, J. S. Gustavsson, and A. Larsson, "High-speed 850 nm VCSELs operating error free up to 57 Gbit/s," *Electron. Lett.*, vol. 49, no. 16, pp. 1021–1023, 2013.

[3] M. P. Tan, S. T. M. Fryslie, J. A. Lott, N. N. Ledentsov, D. Bimberg, and K. D. Choquette, "Error-free transmission over 1-km OM4 multimode fiber at 25 Gb/s using a single mode photonic crystal vertical-cavity surface-emitting laser," *IEEE Photon. Technol. Lett.*, vol. 25, no. 18, pp. 1823–1825, Sep. 15, 2013.

[4] R. Safaisini, E. Haglund, P. Westbergh, J. S. Gustavsson, and A. Larsson, "20 Gbit/s data transmission over 2 km multimode fibre using 850 nm mode filter VCSEL," *Electron. Lett.*, vol. 50, no. 1, pp. 40–42, 2014.

[5] M. Grabherr, R. Jager, R. Michalzik, B. Weigl, G. Reiner, and K. J. Ebeling, "Efficient single-mode oxide-confined GaAs VCSEL's emitting in the 850-nm wavelength regime," *IEEE Photon. Technol. Lett.*, vol. 9, no. 10, pp. 1304–1306, Oct. 1997.

[6] H. Dalir and F. Koyama, "29 GHz directly modulated 980 nm vertical-cavity surface emitting lasers with bow-tie shape transverse coupled cavity," *Appl. Phys. Lett.*, vol. 103, no. 9, pp. 091109-1–091109-4, 2013.

[7] H. Dalir and F. Koyama, "Highly stable operations of transverse coupled cavity VCSELs with enhanced modulation bandwidth," *Electron. Lett.*, vol. 50, no. 11, pp. 823–824, 2014.

[8] H. Dalir and F. Koyama, "High-speed operation of bow-tie-shaped oxide aperture VCSELs with photon–photon resonance," *Appl. Phys. Exp.*, vol. 7, no. 2, p. 022102, 2014.

[9] P. Bardella and I. Montrosset, "A new design procedure for DBR lasers exploiting the photon–photon resonance to achieve extended modulation bandwidth," *IEEE J. Sel. Topics Quantum Electron.*, vol. 19, no. 4, Jul./Aug. 2013. Art. ID 1502408

[10] B. Hawkins, R. A. Hawthorne, III, J. K. Guenter, J. A. Tatum, and J. Biard, "Reliability of various size oxide aperture VCSELs," in *Proc. 52nd Electron. Compon. Technol. Conf.*, 2002, pp. 540–550.

[11] M. T. Johnson, D. F. Siriani, M. P. Tan, and K. D. Choquette, "Beam steering via resonance detuning in coherently coupled vertical cavity laser arrays," *Appl. Phys. Lett.*, vol. 103, no. 20, p. 201115, 2013.

[12] J. J. Raftery, A. J. Danner, J. C. Lee, and K. D. Choquette, "Coherent coupling of two-dimensional arrays of defect cavities in photonic crystal vertical cavity surface-emitting lasers," *Appl. Phys. Lett.*, vol. 86, no. 20, pp. 201104-1–201104-3, 2005.

[13] D. F. Siriani, P. O. Leisher, and K. D. Choquette, "Loss-induced confinement in photonic crystal vertical-cavity surface-emitting lasers," *IEEE J. Quantum Electron.*, vol. 45, no. 7, pp. 762–768, Jul. 2009.

[14] D. F. Siriani and K. D. Choquette, "Implant defined anti-guided vertical-cavity surface-emitting laser arrays," *IEEE J. Quantum Electron.*, vol. 47, no. 2, pp. 160–164, Feb. 2011.

[15] M. T. Johnson, D. F. Siriani, J. D. Sulkin, and K. D. Choquette, "Phase and coherence extraction from a phased vertical cavity laser array," *Appl. Phys. Lett.*, vol. 101, no. 3, p. 031116, 2012.